Biophysics, Vol. 48, No. 4, 2003, pp. 614–623. Translated from Biofizika, Vol. 48, No. 4, 2003, pp. 656–665.

CELL BIOPHYSICS

Cyclic Electron Transport around Photosystem I: An Experimental and Theoretical Study

I. B. Kovalenko[1], D. M. Ustinin[2], N. E. Grachev[2], T. E. Krendeleva[1], G. P. Kukharskikh[1], K. N. Timofeev[1], G. Yu. Riznichenko[1], E. A. Grachev[2], and A. B. Rubin[1]

[1] *Biological Faculty, Moscow State University, Moscow, 119899 Russia*
[2] *Physical Faculty, Moscow State University, Moscow, 119899 Russia*

Received April 28, 2003

Abstract—Electron spin resonance spectroscopy was used to monitor photoinduced changes in the redox state of P700, a photoactive pigment of photosystem I, in isolated *Pisum sativum* chloroplasts. The kinetics of the ESR signal from P700 (ESR signal I) was recorded at different concentrations of exogenous ferredoxin. A kinetic model was developed for ferredoxin-dependent cyclic electron transport around photosystem I. A multiparticle model was built to directly describe electron transfer in multienzyme complexes and restricted diffusion of mobile carriers in individual compartments (stroma, lumen, intramembrane space) of the system. The two models were compared, and a conclusion was made that the spatial organization of the system plays a significant role in shaping the kinetics of redox transitions of P700.

Key words: photosystem I, cyclic electron transport, kinetic model, multiparticle model, ferredoxin

INTRODUCTION

In addition to noncyclic electron transport from water to NADPH, there exists cyclic electron transport in higher plant and alga chloroplasts, which is an antimycin A-sensitive process of charge transfer from the acceptor side of photosystem I to the quinone pool. The physiological role of cyclic electron transport is to generate an additional proton gradient and to protect against oxidative stress on exposure to bright light. Experimental data, including the data of inhibitor analysis, suggest that plastoquinone PQ and the cytochrome b_6/f complex are involved in cyclic electron transport (Fig. 1; [1–4]). The characteristics of cyclic transport in isolated chloroplasts depend significantly on the concentration of added ferredoxin, indicating that this mobile carrier also takes part in this process. However, the question arises of the mechanisms whereby electrons are passed from ferredoxin, a hydrophilic carrier that resides in the stroma, to plastoquinone, whose molecules are hydrophobic and are localized within the thylakoid membrane (Fig. 1). Several schemes of this process have been proposed [4–7], including those implicating the involvement of ferredoxin–quinone reductase, a still unidentified membrane enzyme (Fig. 1). Some evidence suggests that its role may be played by ferredoxin:NADP$^+$ oxidoreductase (FNR), but there are also arguments against this suggestion [1, 2, 5, 8].

In this study, we used electron spin resonance spectroscopy to monitor photoinduced changes in the redox state of P700, a photoactive pigment of photosystem I, over a time interval from 0.1 to 1.0 s. The kinetics of the ESR signal from P700 (ESR signal I) was recorded at different concentrations of added ferredoxin. To describe these data, several kinetic models were constructed based on different schemes of ferredoxin-dependent cyclic electron transport around photosystem I, and the most adequate model was then determined. A multiparticle model was built to directly describe electron transfer in multienzyme

Abbreviations: Fd, ferredoxin; FNR, ferredoxin:NADP$^+$ oxidoreductase; FQR, ferredoxin:quinone reductase; EDTA, ethylenediamine tetraacetic acid disodium salt; HEPES, @N-(2-hydroxyethyl)piperazine-@N′-2-ethanesulfonic acid; Pc, plastocyanin; Phe, pheophytin; PQ, plastoquinone; PQH_2 or QH_2, plastoquinol; PS, photosystem.

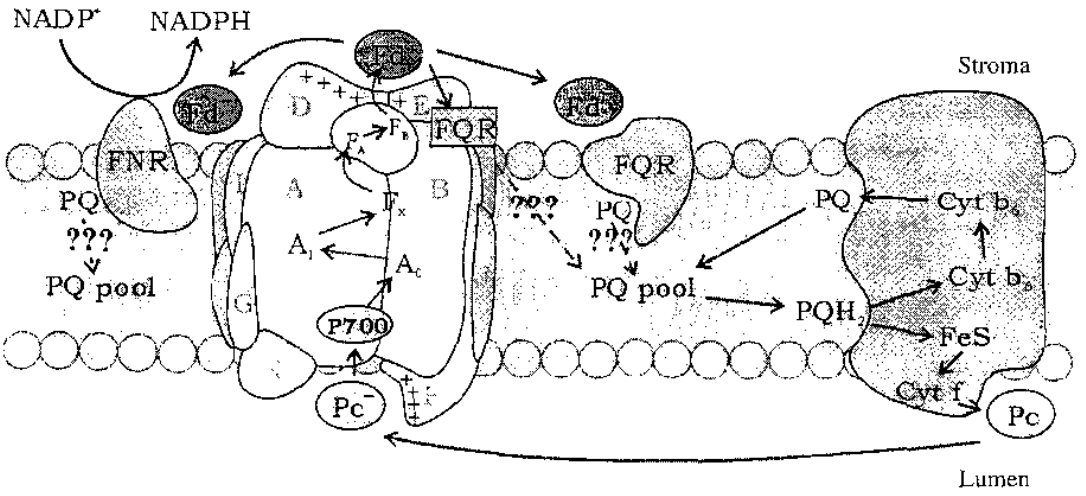

Fig. 1. Organization of cyclic electron transport in chloroplasts. The scheme depicts the thylakoid membrane and the components of the electron transport chain (PS I, FQR, FNR, and cytochrome b_6/f complexes; and mobile electron carriers Pc, Fd, and Q). Question marks indicate where the mechanism of electron transfer is still unclear.

complexes and restricted diffusion of mobile carriers in individual compartments (stroma, lumen, intramembrane space) of the system. This model was compared with the kinetic model, and a conclusion was made that the spatial organization of the system plays a significant role in shaping the kinetics of redox transitions of P700.

EXPERIMENTAL

Thylakoids from leaves of 12-day-old pea seedlings (*Pisum sativum*, cultivar Sovershenstvo) were isolated in 0.4 M sucrose containing 3 mM $MgCl_2$, 2 mM KCl, 1 mM EDTA, and 30 mM HEPES (pH 7.8). The isolated thylakoids were stored frozen in liquid nitrogen containing 20% glycerol. Before experiments, the thylakoids were washed in 0.2 M sucrose containing 6 mM $MgCl_2$ and 30 mM Tricine (pH 7.6). Ferredoxin was isolated from pea leaves as described by Mutuskin *et al.* [9]. The photoinduced ESR signal I ($g = 2.0025$) from $P700^+$ was recorded with a PC-interfaced RE-1307 X-band spectrometer (NTO AN, Russia). The data were stored as averages of every ten replicate measurements. Light from a KGM-300 halogen lamp passed to a cuvette through a set of heat-blocking filters. The reaction mixture was 0.1 ml in volume and contained 50 mM Tricine (pH 7.5), 5 mM $MgCl_2$, 6 mM glucose, 2 mM NH_4Cl, 400 U/ml catalase, 40 μM ferredoxin (unless otherwise indicated), and thylakoids (chlorophyll content, 0.1 mg). To create a pool of reduced ferredoxin required for cyclic electron transport, the thylakoids in the reaction mixture were illuminated with intense white light from a incandescent lamp for 30 s. On the 30th s of illumination, 10 μM diuron was added to the reaction mixture to block electron transport from photosystem II. To make the reaction mixture anaerobic, it was placed under argon and supplemented with 4 U/ml glucose oxidase. The agents whose effects were studied were added after diuron. The sample prepared in this way was transferred into a spectrometer cuvette and illuminated for 1.5 s, after which the kinetics of dark reduction of photooxidized $P700^+$ was recorded. The kinetic data were analyzed using a nonlinear regression routine of the Mathcad 7 program.

RESULTS

Experimental Data

Typical examples of the experimental kinetics of the ESR signal I are shown in Fig. 2. Switching on the light causes P700 oxidation, as judged by a sharp rise in the amplitude of this signal to some stationary level. The kinetics of the subsequent dark reduction was fit well with a sum of two exponential functions. The table summarizes the kinetic parameters of the fast and the slow phases of this process obtained by deconvoluting the experimental curves into two exponential components. Their amplitudes, time constants, and the contribution of the fast component to the total signal were determined for several concentrations of

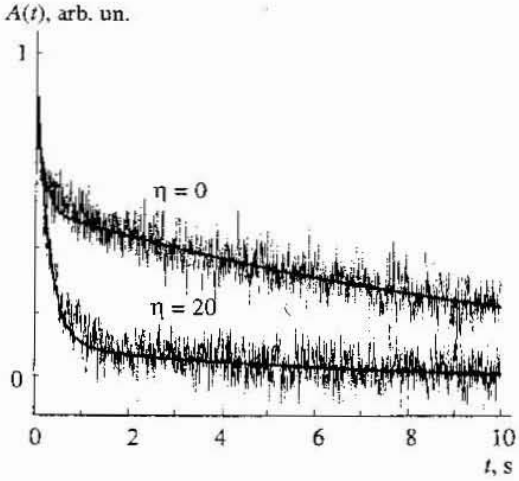

Fig. 2. Temporal evolution of the photoinduced ESR signal I from cation radical P700 in the dark for two concentrations of exogenous ferredoxin. Solid lines are a bi-exponential fit to the experimental curves: $A(t) = A_1\exp(-k_1t) + A_2\exp(-k_2t)$, where A_1 and A_2 are the amplitudes of the fast and slow components, respectively; k_1 and k_2 are their time constants (see table); and η is the concentration ratio of exogenous Fd to PS I.

added ferredoxin. As can be seen in the table, the characteristic time was about 200 ms for the fast component and 2–5 s for the slow component. At higher concentrations of added ferredoxin, the relative contribution of the fast component to $P700^+$ reduction was greater. However, the characteristic time of the fast component (reciprocal of the time constant) varied little with the ferredoxin concentration. In contrast, the time constant of the slow component was larger at higher ferredoxin concentrations. In other words, ferredoxin accelerated the slow phase. This observation supports the suggestion put forward by Scheller [7] that the slow phase of P700 reduction is accounted for by the nonuniform donor environment and only brings this process to completion. To interpret the experimental data formally, we built kinetic models.

Kinetic Model: Description and Results of Modeling

The kinetics of the ESR signal I is determined by the following processes in the system under study. Under action of light, photosystem I catalyzes oxidation of plastocyanin (Pc) on the lumenal side of the thylakoid membrane and reduction of ferredoxin on its stromal side. They are followed by oxidation of ferredoxin and reduction of the plastoquinone pool. Given that ferredoxin molecules are localized within the stroma and that plastoquinone is a hydrophobic carrier residing in the lipid layer of the membrane, these events are likely to be mediated by membrane exposure of a protein with FQR activity to the stroma. The subsequent oxidation of plastoquinone involves the cytochrome b_6/f complex and results in the reduction of plastocyanin, which is localized in the lumen; (Fig. 1).

We built a set of increasingly complex kinetic models, with most detailed of them taking account of the processes of ferredoxin docking on the acceptor side of photosystem I, the involvement of the cytochrome transmembrane complex in redox transitions of plastoquinone, interaction of the latter with the cytochrome complex, and the two-electron nature of this carrier. The scheme of the most complete model is presented in Fig. 3. This model incorporates even a hypothetical FQR complex.

Kinetic parameters of dark reduction of photooxidized $P700^+$ in pea thylakoids under anaerobic conditions, as determined for different concentrations of added ferredoxin

Concentrations of added ferredoxin, μM	A_1, arb. un.	k_1, s^{-1}	τ_1, s	A_2, arb. un.	k_2, s^{-1}	τ_2, s	$A_1/(A_1 + A_2)$
0	0.240	6.85	0.146	0.361	0.181	5.51	0.33
5	0.166	4.93	0.203	0.276	0.218	4.57	0.35
10	0.458	4.49	0.222	0.192	0.514	1.94	0.74
15	0.593	4.28	0.233	0.163	0.428	2.33	0.80
20	0.656	4.23	0.236	0.159	0.464	2.15	0.86

Note: A_1 and A_2 are the amplitudes of the fast and slow components of the signal, respectively; k_1 and k_2 are their time constants; and τ_1 and τ_2 are their characteristic times; the last table column shows the contribution of the fast component to the total signal.

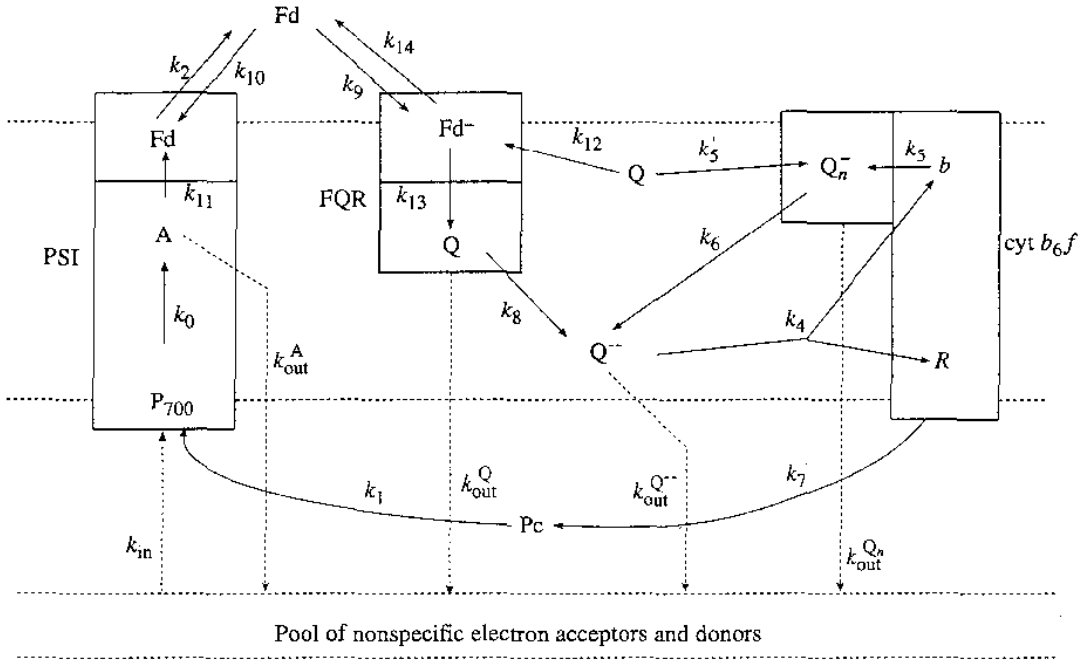

Fig. 3. Scheme for the kinetic model of cyclic electron transport around photosystem I. Boxes stand for PS I, FQR, and cytochrome b_6/f complexes; P700, pigment of the PS I reaction center; *A*, generalized acceptor; *R*, Rieske center; *b*, high-potential cytochrome b_h; Fd, ferredoxin; Pc, plastocyanin; Q, plastoquinone; Q^{--}, plastoquinol; Q_n, semiquinone at the *n*th site of the cytochrome complex (on the outer side of the membrane). Arrows indicate electron transport pathways; k_{in}, k_{out}, k_1, ..., k_{13}, and k_{14} are the rate constant for the respective reactions of electron transfer. Dashed lines depict the boundaries of the thylakoid membrane and the boundary of the pool of nonspecific electron acceptors and donors.

Electron transfer within multienzyme complexes was described by equations for the probabilities of particular states of these complexes. In the model, we used the reduced schemes of the states of the complexes. We did not go into details of electron transfer within the complexes, because the characteristic times of these stages are much shorter that the characteristic times of the processes that we observed in the experiments (0.1 s). Interaction of the complexes with mobile carriers was described by equations derived from the law of mass action [10, 11].

For the photoreaction center complex of photosystem I, the scheme of its states is given in Fig. 4a. This complex is supposed to comprise the primary electron donor P700, the generalized acceptor, and the ferredoxin binding site. The cytochrome b_6/f complex (Fig. 4b) is regarded as consisting of two catalytic components—the Rieske center and the high-potential cytochrome b_h—and the binding site for plastoquinone Q_n. Electron transport through the cytochrome complex is known as the Q cycle. Ferredoxin bound to the complex is thought to be in dynamic equilibrium with free ferredoxin in solution. We assumed that a separate protein complex exists that acts as FQR (Fig. 4c) and for which six states are possible.

The kinetic model corresponding to the scheme in Fig. 3 is a set of 26 ordinary differential equations. The model variables are the probabilities of particular states of the complexes and the relative concentrations of reduced mobile carriers (plastocyanin, ferredoxin, and plastoquinone). The initial conditions were specified according to the stationary electron distribution in the absence of light. The set of model equations was solved numerically using the Model Vision Studium program [12].

The model parameters were chosen from the literature data. The "light" constant k_0 was assumed to be proportional to the light intensity I: $k_0 = I\sigma$, where σ is the effective section of light absorption by photosystem I. For a light intensity of 500 W/m^2 (our experimental conditions), $k_0 = 250$ s^{-1} [13–15]. As in the study by Hope *et al.* [16], the rate constants k_4, k_5, k_6, and k_7 for the reactions in the cytochrome complex were set to 50, 457, 10 000, and 4000, respectively. For the reaction between plastocyanin and P700, the

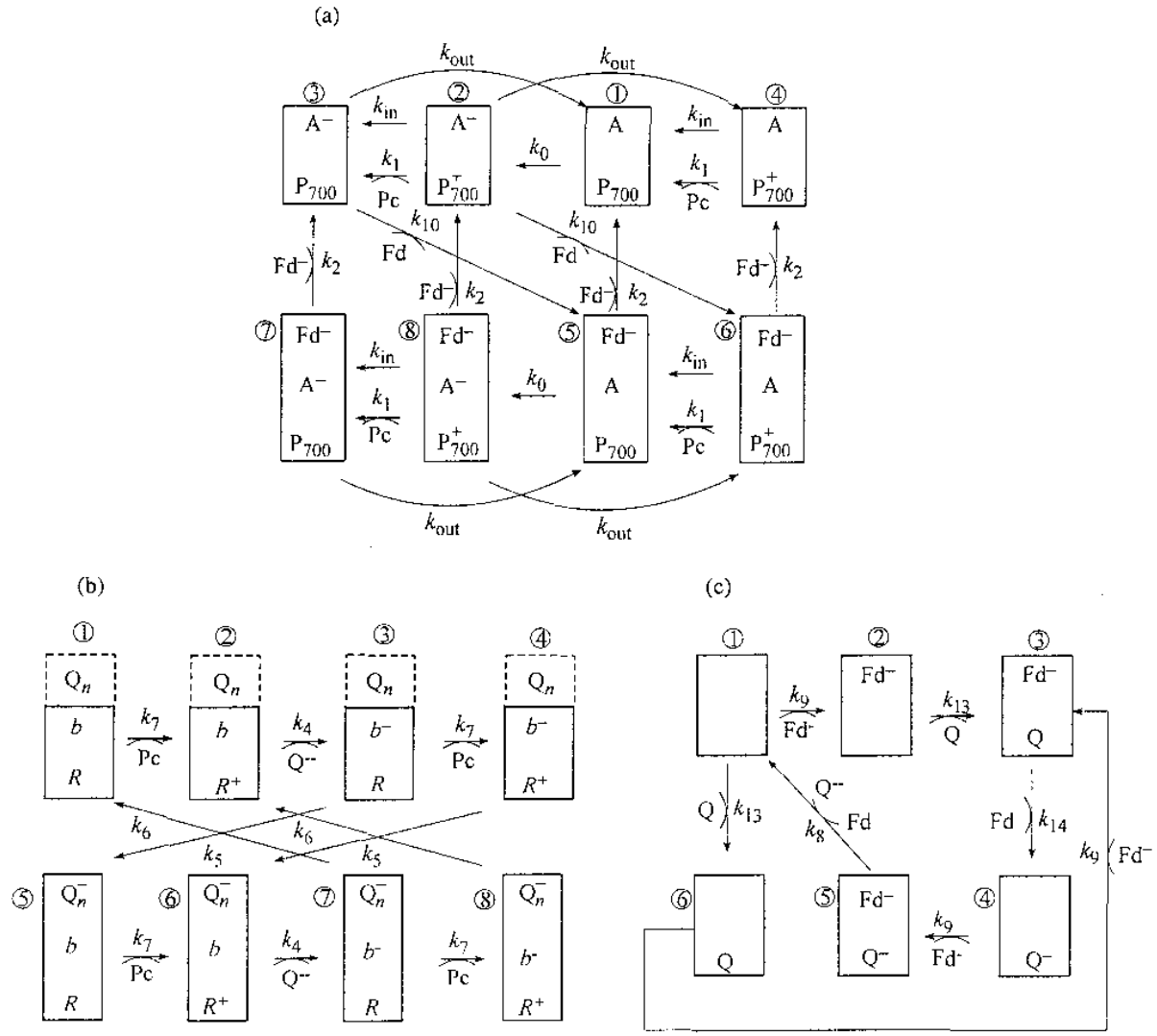

Fig. 4. Scheme of the states of the complexes involved in cyclic electron transport around photosystem I: (a) photoreaction center of PS I, including the pigment P700 (P700) and the generalized acceptor (*A*); (b) cytochrome b_6f complex, including the Rieske center (*R*), high-potential cytochrome *b* (*b*) and plastoquinone at the *n*th binding site of the complex on the outer surface of the membrane (Q_n); and (c) FQR complex. Each box stands for a particular state of a particular complex, which is determined by the redox states of individual electron carriers contained in that complex. Arrows indicate the electron transport pathways; k_{in}, k_{out}, k_1, ..., k_{13}, and k_{14} are the rate constant for the respective reactions of electron transfer.

rate constant (k_1) was set to 4000 [16, 17]. The value of the rate constant k_{11} ($k_{11} = 50\,000$) for the reaction between photosystem I and ferredoxin was taken from [18]. The other reaction constants were varied.

The model kinetics of redox transitions of P700 is shown in Fig. 5. These curves are similar to the experimental ones (Fig. 2) in that the fast phase of $P700^+$ reduction, which is due to cyclic electron transport, can be approximated well with a single exponent. Moreover, in the model (Fig. 5), as in the experiment (Fig. 2), the reduction of $P700^+$ by virtue of cyclic electron transport does not proceed to completion, because a small fraction of electrons remain "trapped" after illumination in the stroma in the form of reduced molecules of semiquinone and ferredoxin, or by other groups. It is natural that P700 would be reduced with time from nonspecific donors. Therefore, the entire curve for the reduction of photooxidized P700 can be approximated with a sum of two exponential functions.

Analysis of the model results shows that the amplitude and the contribution of the fast component to the dark reduction of P700 depend on the concentration of added ferredoxin (Fig. 5). Let the extent of reduction of the latter be fixed. Then, given that diuron blocks the electron influx from photosystem II and the water-splitting complex (which is a natural electron donor), we obtain that the total number of electrons in the system would increase with the ferredoxin concentration. Hence, more electrons would be involved in the system of cyclic transport around photosystem I. As a result, the amplitude of the fast component of P700 reduction and thereby the relative contribution of this component to the overall effect would grow. However, the fast-phase rate of P700 reduction would not increase, because it depends on the transfer rates of electrons at various stages of the cyclic pathway, which remain unchanged.

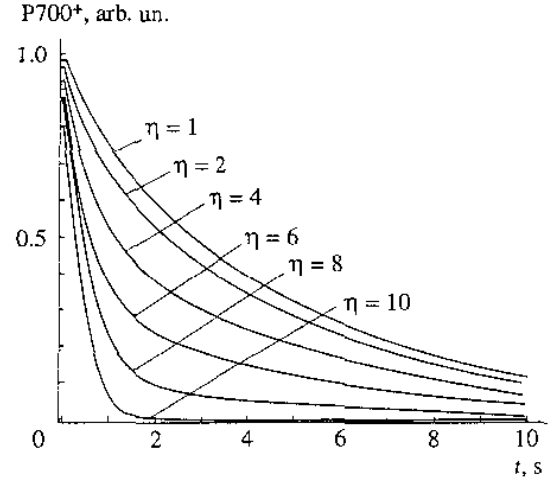

Fig. 5. Time course of dark reduction of photooxidized P700, as calculated in the kinetic model for different values of the Fd-to-PS I concentration ratio η.

The slow phase of the reduction process can be described in the model by incorporating either a weak flux through the system or a large nonspecific electron pool, from which electrons required for the completion of P700 reduction may be taken. The rate of this slow nonspecific phase is likely to increase with the number of electrons in the system (table).

What is the nature of the slow phase? The photoactive pigment of the photosystem I reaction center is a powerful oxidant [18, 19]. Therefore, when the reduced specific donor plastocyanin is absent, electrons can be transferred, albeit slowly, to oxidized P700 from other, nonspecific donors. As suggested by Scheller [7], the slow phase of P700 reduction reflects the ability of $P700^+$ to remove electrons from the surrounding molecules, because this reaction can proceed even in the presence of oxygen. Scheller [7] also indicates that the slow phase resembles the reaction observed in the isolated photosystem I complex. The slow phase has also been described in the reduction of P700 oxidized with a flash of light [20]. However, Hope *et al.* [20] refer to this reaction as nonphysiological. The results obtained with our model support these suggestions.

Direct Modeling of Cyclic Electron Transport around Photosystem I

The kinetic approach to modeling of primary photosynthetic processes has a number of flaws. The main flaw is the inability to take into account the spatial structural heterogeneity of the system. The use of the law of mass action is justifiable in modeling the interaction of isolated fragments with exogenous donors and acceptors in solution. Only in this case can the system be relatively homogeneous. However, in the native thylakoid membrane, multienzyme complexes interact with mobile carriers in different compartments of the system (with ferredoxin, in the stroma; with plastoquinone, in the lipid bilayer of the membrane; with plastocyanin, in the lumen; Fig. 1). At least in two of these compartments, namely, in the intramembrane space and the lumen, free diffusion is impossible because of the size limitations: the protein complexes often span the entire compartment where they are embedded.

An *a priory* assumption that diffusion is free in the stromal space may also be invalid. Although the stromal space is large, the conditions for free diffusion are not satisfied near the membrane because of the presence of the protein complexes and their reaction centers. With a kinetic approach to modeling, it is difficult to describe docking, conformational rearrangements, and other processes, in which the spatial organization of interacting elements may affect their function. All these processes can be simulated by means of "direct," or multiparticle modeling.

In this study, we built a multiparticle model of cyclic electron transport around photosystem I, which includes all the components shown in Fig. 6.

The model is organized as a three-dimensional stage (Fig. 6) made of the thylakoid membrane, the intrathylakoid space, and the lumen and filled with pigment–protein complexes (photosystem I, the

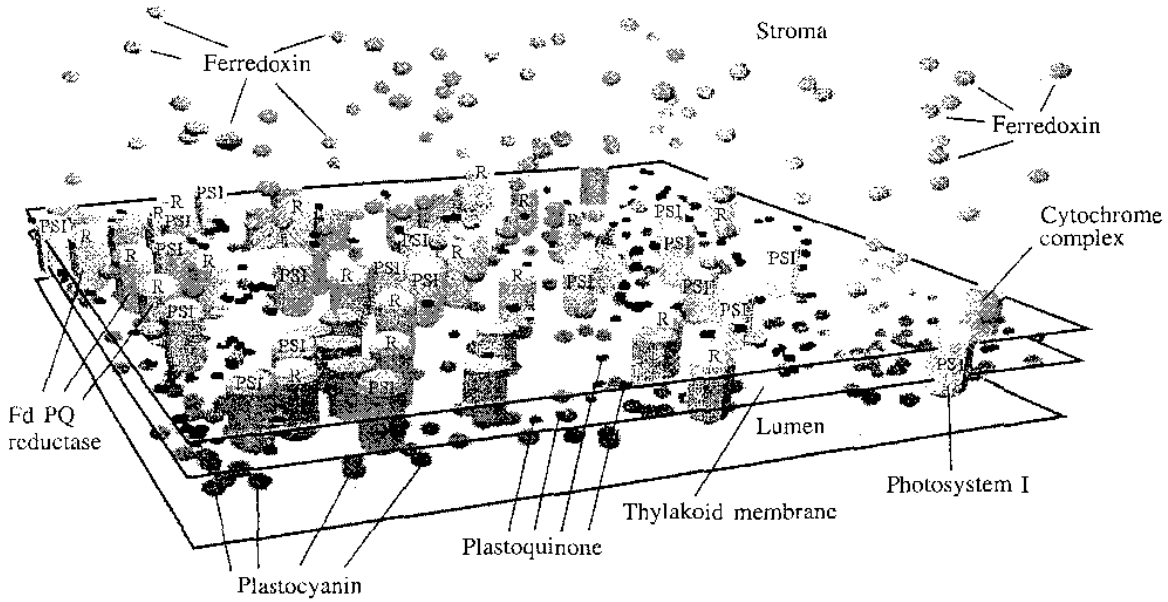

Fig. 6. Visualization of the three-dimensional stage for the "direct" model of cyclic electron transport around photosystem I. Segments of the thylakoid membrane, lumenal space, and stromal space are shown.

cytochrome complex, and FQR) and mobile electron carriers (plastocyanin, ferredoxin, and plastoquinone).

To model the motion of plastocyanin, ferredoxin, and plastoquinone in their respective compartments, we used the mathematical formalism of the theory of Brownian motion, taking into account the constraints imposed by the organization of the model stage specified above. In our model, we assume that particles move in a viscous medium under the action of random forces arising during collisions with the molecules constituting the medium. As shown in [21], their motion can be simulated with the Langevin equation, describing how each particular coordinate varies with time under the action of a random force:

$$\xi \frac{dx}{dt} = f(t),$$

where ξ is the friction coefficient, and $f(t)$ is a random force. The random force has a normal distribution with mean 0 and variance $2kT\xi$, where k is the Boltzmann constant, and T is temperature. The friction coefficient for a spherical particle of radius a reads

$$\xi = 6\pi\eta a,$$

where η is the medium viscosity. This equation was solved numerically using the adaptive time step scheme. Specifically, at any given step, the time increment was chosen so that we had the square root of variance of particle displacement (root-mean-square displacement) approximately equal to one-tenth of the mobile carrier diameter. The choice of the time step size in this way ensures a reasonable accuracy and an acceptable computation time. At the right and left boundaries, toroidal (periodic) conditions were imposed. We also took into account the possibility of particle repulsion from physical surfaces, including those of the membrane and protein complexes. Any moving particle could either carry an electron or not. In animation, particles with and without electrons came in different colors.

The states of the complexes, the mechanisms of their interaction with the carriers, laws of motion for carriers were specified according to a set of certain rules. At the level of detail used, these rules were as follows (Fig. 6). The inner space of the thylakoid (lumen) is bounded with the membrane. Within the lumen, there are moving particles of plastocyanin, which are capable of carrying an electron. Outside the thylakoid (in the stroma), there are moving particles of ferredoxin, which are also capable of carrying an electron. The membrane contains integral protein complexes (photosystem I, cytochrome, and FQR) spanning it. Their concentrations and sizes were estimated from the literature data [18, 22, 23]. The photosystem I complex can accept an electron from

plastocyanin, transfer it under the action of light across the membrane, and pass to ferredoxin. This mechanism does not operate in the dark. Therefore, the probability of electron transfer from P700 to *A* was assumed proportional to the light intensity in the model. The next steps of cyclic electron transport are the oxidation of ferredoxin in the stroma and the reduction of plastoquinone in the membrane, in which the FQR complex is involved. Oxidation of plastoquinone and reduction of lumenal plastocyanin proceed by the Q-cycle mechanism and involve the transmembrane cytochrome complex [18]. In its turn, plastocyanin is a donor for the photoactive pigment P700 (which is the donor part of the photosystem I complex). Thus, the cycle is closed.

The mechanism of electron transfer is as follows: if a mobile carrier moving by Brownian diffusion (chaotically) approaches the protein complex by a distance shorter than the effective radius of their interaction, there is a probability of the carrier docking to the complex. The effective radius of interaction is a model parameter that characterizes the maximum distance from which docking is possible. The effective radii of interaction were set equal to the sizes of interacting proteins. This assumption means that docking could take place only upon their collision. The probability of docking is also a model parameter. The effective radii and the probabilities of docking of mobile carriers to the complexes can be assessed by studying their effects in the kinetic constants of interaction of, for example, plastocyanin with photosystem I. Knowing (from the experimental data) the constant for P700 reduction (interaction of P700 with plastocyanin), we can choose the effective radius and the docking probability in a range allowing the frequency of individual reduction events to agree well with the experimentally determined value of the kinetic constant (the characteristic time) of P700 reduction. After docking, some time *dt* (also a model parameter) passes during which the complex between photosystem I and plastocyanin undergoes conformational changes required for electron transfer from plastocyanin to photosystem I. Thereafter, the oxidized plastocyanin resumes Brownian motion.

The direct model and the kinetic model described above are capable of reproducing the kinetic curves of dark reduction of photooxidized P700 obtained experimentally and can be used in kinetic studies of the other model variables. In addition, direct

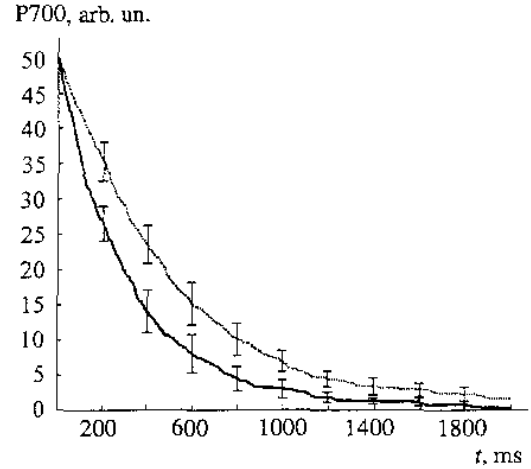

Fig. 7. Kinetics of dark reduction of photooxidized P700, as calculated in the multiparticle model for cases when PS I, cyt b_6/f, and FQR are uniformly distributed in the membrane (dashed line) and when PS I, cyt b_6/f form a complex (solid line). Each kinetic curve is an average of ten replicates of the numerical experiment.

modeling makes it possible to study how the characteristics of the system depend on the spatial distribution of pigment–protein complexes in the membrane, the geometric parameters (shape and size) of the carriers, the parameters of docking of mobile carriers to molecular complexes, and on other characteristics of the system.

By way of example, Figure 7 shows two curves of dark reduction of photooxidized P700 calculated in the direct model. The dashed line corresponds to the uniform distribution of the protein complexes (PS I, cyt b_6/f, and FQR) over the thylakoid membrane. The solid line corresponds to the case when the photosystem I and the cytochrome b_6/f complexes lie close to each other and form a supercomplex. In both cases, the kinetic curves are approximated well with a single exponential function. The formation of a supercomplex results in a shorter characteristic time of dark reduction, because there is no need for plastocyanin to diffuse from the cytochrome complex to photosystem I in this case. The possibility of the existence of such a supercomplex is discussed in the study by Bendall and Manasse [2]. Note that the kinetics of dark reduction of photooxidized P700 calculated for the random spatial distribution of all the three protein complexes coincides with that calculated for the case when only the cytochrome complex is assumed to be distributed randomly, whereas the other two complexes occur in pairs. This result may indicate that the

limiting stage is electron transfer from plastoquinone to plastocyanin via the cytochrome b_6f complex.

The opportunities afforded by the new type of modeling of primary photosynthetic processes in the thylakoid membrane will be assessed more comprehensively in future studies.

DISCUSSION

It is common to use a kinetic approach in modeling the processes of electron transfer in photosynthesis. To simulate electron transfer in multienzyme complexes, equations for the probabilities of particular states of the complexes are employed, along with equations describing interaction of the complexes with mobile carriers that are derived from the law of mass action [10, 11, 24]. We used this approach to simulate electron transfer in isolated fragments of photosystem I in the presence of exogenous donors and acceptors. The models developed and the results of identification of the parameters of the system were reported in our previous publications [10, 25, 26]. It was admissible to derive equations describing redox reactions of exogenous mobile carriers with photosynthetic reaction center complexes from the law of mass action because they freely diffused and interacted in solution. However, the spatial organization of the native thylakoid membrane is such that the assumption of free diffusion does not hold.

In recent years, considerable data has accumulated concerning the structure and regulation of photosynthetic processes that has yet to be brought together within a unifying functional framework. The methods of modern object-oriented programming and ever-increasing software and hardware availability make it possible, at least in principle, to integrate the structural and kinetic notions. In this connection, "direct" modeling seems very promising. In this study, we attempted for the first time to describe cyclic electron transport around photosystem I by this method.

Direct modeling allows the researcher to test the validity of the approaches used in kinetic modeling and to assess the range of applicability of the latter. The models developed by this method make it possible (i) to analyze the effects of the structural characteristics of the system on the rate constants and other parameters of kinetic models, and (ii) to clarify the role of the spatial heterogeneity of the system, for example, of the nonuniform distribution of multienzyme complexes over the thylakoid membrane. These questions, as well as the role and the effects of electric and electrochemical potentials, which have not been addressed in the direct model proposed, are the subject of future research.

ACKNOWLEDGMENT

The work was supported by the Russian Foundation for Basic Research (projects nos. 03-04-49 048 and 01-07-90 131).

REFERENCES

1. Krendeleva, T.E., Kukarskikh, G.P., Timofeev, K.N., Ivanov, B.N., and Rubin, A.B., *Dokl. Ross. Akad. Nauk*, 2001, vol. 379, no. 5, pp. 1–4.
2. Bendall, D.S. and Manasse, R.S., *Biochim. Biophys. Acta*, 1995, vol. 1229, pp. 23–38.
3. Moss, D.A. and Bendall, D.S., *Biochim. Biophys. Acta*, 1984, vol. 767, pp. 389–395.
4. Heimann, S. and Schreiber, U., *Plant Cell Physiol.*, 1999, vol. 40, pp. 818–824.
5. Cleland, R.E. and Bendall, D.S., *Photosynth. Res.*, 1992, vol. 34, pp. 409–418.
6. Hosler, J.P. and Yocum, C.F., *Biochim. Biophys. Acta*, 1985, vol. 808, pp. 21–31.
7. Scheller, H.V., *Plant Physiol.*, 1996, vol. 110, pp. 187–194.
8. Allen, J.F., *TRENDS in Plant Science*, 2003, vol. 8(1), pp. 15–19.
9. Mutuskin, A.A., Pshenova, K.V., and Kolesnikova, P.A., *Biokhimiya*, 1966, vol. 31, pp. 924–927.
10. Riznichenko, G.Yu., *Itogi Nauki i Tekhniki, Ser.: Biofizika*, Moscow: VINITI, 1991, p. 31.
11. Rubin, A.B., *Biofizika* (Biophysics), Moscow: Knizhnyi Dom Universitet, 2000, vol. 2.
12. Ben'kovich, E.S., Kolesov, Yu.B., Senichenkov, Yu.B., *Prakticheskoe modelirovanie dinamicheskikh sistem* (Practice of Modeling of Dynamical Systems), St. Petersburg: BKhV-Peterburg, 2002.
13. Dau, H., *Photochem. Photobiol.*, 1994, vol. 60, pp. 1–23.
14. Lebedeva, G.V., Belyaeva, N.E., Demin, O.V., Riznichenko, G.Yu., and Rubin, A.B., *Biofizika*, 2002, vol. 47, no. 6, pp. 1044–1058.

15. Schreiber, U. and Neubauer, C., *Z. Naturforsch*, 1987, vol. 42c, pp. 1255–1264.

16. Hope, A.B., Liggins, J., and Matthews, D.B., *Aust. J. Plant Physiol.*, 1989, vol. 16, pp. 353–364.

17. Hope, A.B., *Biochim. Biophys. Acta*, 2000, vol. 1456, pp. 5–26.

18. Malkin, R. and Niyogi, K., *Biochemistry & Molecular Biology of Plants*, Buchanan, B., Gruissem, W., and Jones, R., Eds., American Society of Plant Physiologists, 2000, pp. 568–628.

19. *Photosynthesis*, Govindjee, Ed., New York: Academic Press, 1982, vol. 1. Translated under the Title *Fotosintez*, Moscow: Mir, 1984, vol. 1.

20. Hope, A.B., Huilgol, R.R., Panizza, M., Thompson, M., and Matthews, D.B., *Biochim. Biophys. Acta*, 1992, vol. 1100, pp. 15–26.

21. Doi, M. and Edwards, S.F., *The Theory of Polymer Dynamics*, Oxford: Clarendon, 1986. Translated under the Title *Dinamicheskaya teoriya polimerov*, Moscow: Mir, 1999.

22. Albertsson, P.-A., *TRENDS in Plant Science*, 2001, vol. 6(8), pp. 349–354.

23. Albertsson, P.-A., *Recent Res. Devel. Bioener.*, 2000, vol. 1, pp. 143–171.

24. Riznichenko, G.Yu., Lebedeva, G.V., Demin, O.V., Belyaeva, N.E., and Rubin, A.B., *J. Biol. Phys.*, 1999, vol. 25, pp. 177–192.

25. Riznichenko, G.Yu., Vorobjeva, T.N., Khrabrova, E.N., and Rubin, A.B., *Photosynthetica*, 1990, vol. 24(3), pp. 37–51.

26. Vorob'eva, T.N., Krendeleva, T.E., Riznichenko, G.Yu., Shaitan, K.V., and Rubin, A.B., *Mol Biol.*, 1983, vol. 17, pp. 82–91.